1

Challenges toward monocycle free electron lasers

Shortening the laser pulse length, ultimately toward the monocycle time scale, is one of the most important subject in the laser technology. Although this is also the case for free electron lasers (FELs), there is a fundamental and theoretical lower limit to the attainable pulse length in FELs, which comes from the so-called slippage effect intrinsic to the FEL amplification process. In this paper, a new FEL concept, which has been proposed to overcome the theoretical limit and realize monocycle FELs, is explained together with reviewing two schemes to implement the concept in the actual FEL system.

Keywords: Free Electron Lasers, Short Pulse

1. Introduction

When we take a picture of fast-moving objects, such as a flying hummingbird, the shutter speed of a camera should be sufficiently high. Nowadays, the highest shutter speed of conventional cameras is at most 1 ms, and thus it is difficult to take a clear picture if the target object is moving with the typical time scale shorter than 1 ms. This discussion also applies to observation of ultrafast dynamics using a pulsed laser; the pulse length should be shorter than the typical time scale of the target phenomena, and thus shortening the pulse length is one of the most important subjects in the laser development. Recent advancement of the laser technology has made it possible to generate a laser pulse with the pulse length shorter than 10 fs, which is quite attractive to many applications in various research fields.

It is obvious that the shortest pulse length scales as the wavelength of light and ultimately gets down to one wavelength or "monocycle", in which case the light wave oscillates just once while it illuminates the target object. To generate the monocycle laser pulse as mentioned above, we have two requirements to be satisfied. First, the spectral bandwidth of laser amplification should be broad enough. Second, the broadband light should be superimposed coherently in time and space. In long-wavelength regions such as infrared and visible ones, laser media and optical elements with the functions described above are nowadays available, and thus generation of monocycle laser pulses has become a mature technology. This makes it possible to generate an intense ultrashort laser pulse with the pulse length less than 10 fs, with which ultrafast dynamics having the same time scale can be investigated. Recently, technologies known as the high harmonic generation (HHG) have made it possible to extend the available wavelengths of the monocycle pulse toward the vacuum ultraviolet regions, and the attosecond monocycle pulses with the pulse length of hundreds of attoseconds or shorter have become available [1].

To further shorten the pulse length, we need to shorten the wavelength of lasers; it is obvious, however, that simply extending the above conventional schemes may not lead to a drastic change in the available wavelength of lasers. This is the reason why free electron lasers (FELs) have been developed and become a powerful tool

2

in scientific research fields using x rays [2–4]. Even so, "monocycle FELs", which may significantly shorten the pulse length, have not yet been realized, because of many technical and theoretical reasons. Among them, the most fundamental one is the FEL pulse lengthening due to the so-called optical slippage in undulators. The purpose of this paper is to introduce a new FEL concept recently proposed to counteract the slippage effect in undulators, and to review a few schemes to implement the concept toward realization of the monocycle FELs.

2. Slippage and Pulse Lengthening in FELs

The optical slippage in FELs refers to the fact that electrons moving along a sinusoidal trajectory in an undulator are left behind from radiation emitted by themselves. In other words, the radiation goes ahead of the electrons, or slips out of them by the distance of λ while the electrons travel one undulator period, which depends on the undulator period, undulator field strength and electron energy. Because the radiation with the wavelength λ can interact with the electrons continuously to exchange energy with them, the electron energy is modulated with the period of λ, which is then converted to density modulation with the same period. To be more specific, the electrons form a set of local bunches, which are shorter than λ and are regularly arranged with the interval of λ. This is the so-called microbunch, and the radiation intensity is significantly enhanced compared to the spontaneous radiation, because individual electrons contained in the microbunch emit radiation coherently.

As explained above, the laser medium of FELs is the electron beam, or more specifically, the microbunched electron beam, and thus the pulse length of FEL radiation roughly corresponds to the length of the microbunched domain in the electron beam. In other words, the pulse length can be shortened by shrinking the microbunched domain. Thus, realization of monocycle FELs seems to be possible if a single microbunch is created in the electron beam; in practice, this is not true. Because of the slippage effect, the emitted radiation slips out of the microbunch while the electron beam travels the undulator, and the radiation pulse linearly expands according to the number of undulator periods, which is schematically illustrated in Fig. 1(a).

3. Counteracting the Slippage

The pulse lengthening due to the optical slippage, which has been mentioned in the previous section, has been the biggest obstacle to realization of the monocycle FELs. Although this problem can be solved by using a single period undulator to generate coherent radiation, the resultant peak intensity will be much lower than what is available in normal FELs.

To overcome the above difficulty, a new scheme has been proposed [5], which is based on interference between light waves of coherent radiation. In the proposed
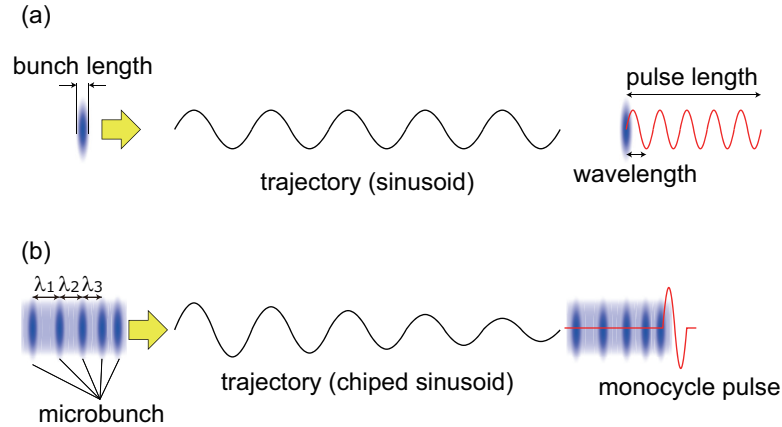
Fig. 1. Emission of coherent radiation (a) by a single microbunch passing through a normal undulator and (b) by CM passing though a tapered undulator.

scheme, an electron beam with the microbunch, whose interval is irregularly arranged, is injected to an undulator with the field strength varying along the longitudinal axis, as illustrated in Fig. 1(b). What is important in this scheme is that the n-th interval of the microbunch (λ_n) should be identical to the slippage length at the n-th period of the undulator. In the simplest case, λ_n linearly changes as n, and the microbunch is referred to as being "chirped", while the undulator is "tapered". As explained in what follows using Fig. 2, which plots the electron current (j) and radiation field (E) as a function of the longitudinal coordinate (s), the pulse length of coherent radiation emitted from the chirped microbunch (CM) can be controlled by tuning the chirp rate, and it can be reduced down to monocycle, if the chirp rate is strong enough.

Figure 2(a) shows the current profile of CM composed of 11 bunches whose interval ($\lambda_1 \sim \lambda_{10}$) linearly changes. Note that these intervals correspond to the slippage length at the n-th period of the tapered undulator.

Figure 2(b) shows the field profile of radiation emitted by the electron beam after it passes through the 1st undulator period. As found in this figure, the electron beam emits coherent radiation whose temporal profile is similar to its current profile, when it travels one undulator period. It should be also mentioned that the radiation waveform is located λ_1 ahead of the electron beam because of the slippage effect. The light pulse indicated by an arrow (hereinafter referred to as a resonant pulse) is generated by the local bunch located at the tail end of CM, which is indicated by the dotted line and is defined as the origin of s. The resonant pulse is located at $s = \lambda_1$ after the 1st period.

Figure 2(c) shows the field profile after the electron beam passes through the 2nd period. The solid line shows the profile generated at the 1st period, while the dotted line shows that at the 2nd period. The resonant pulse is located at $s = \lambda_1 + \lambda_2$,

4
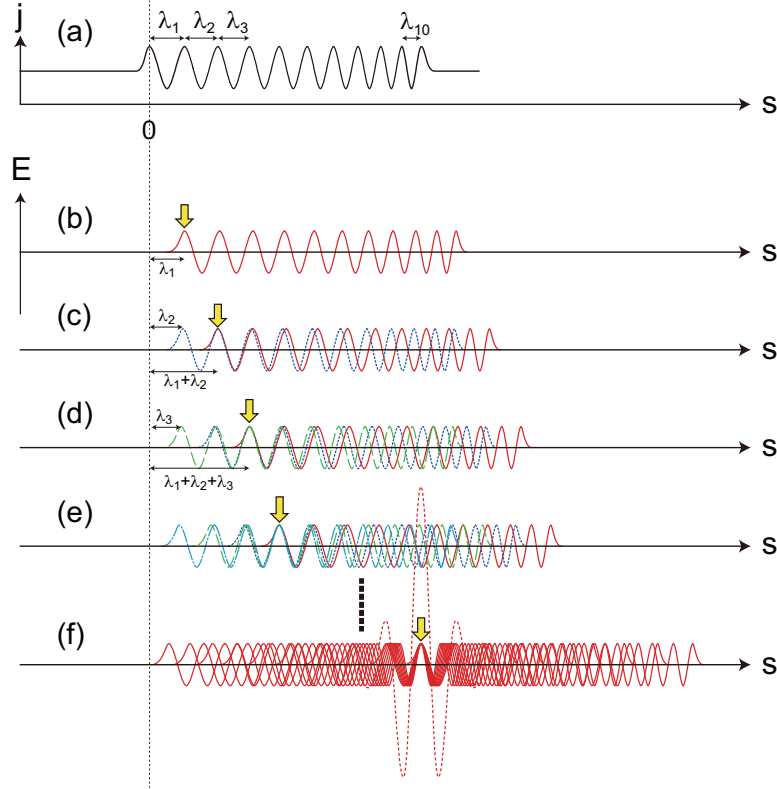
Fig. 2. Mechanism to suppress the pulse lengthening due to the optical slippage by means of CM: (a) current profile of CM, (b∼f) field profile of radiation after the 1st, 2nd, 3rd, 4th and 10th periods, respectively.

because the slippage length at the 2nd period is λ_2 but not λ_1. It is obvious that the radiation is completely in phase only at the position of the resonant pulse.

The above conditions hold after the electron beam passes through the 3rd and 4th periods, as shown in Figs. 2(d) and (e), where the dashed and chain lines show the field profiles generated at the 3rd and 4th periods, respectively.

By repeating the above discussion, it is easy to understand that the field profiles generated after the 10th periods are given in solid lines in Fig. 2 (f). Summing up all the solid lines gives rise to the field profile shown in the dashed line, in which the intensity is enhanced at the resonant pulse (constructive interference), while those at other positions are weakened (destructive interference). As a result, the pulse length can be controlled by adjusting the variation (chirp) rate of λ_n, and a monocycle radiation pulse can be ultimately generated if it is strong enough.

The above mechanism to counteract the slippage effect is explained in a mathematical manner as well. The field profile of coherent radiation, $E(t)$, emitted by CM, is given by convoluting two functions $n(t)$ and $E_s(t)$, where $n(t) = n_0[1+bf(t)]$

denotes the electron distribution function and $E_s(t) = E_0 g(t)$ denotes the electric field of radiation emitted by a single electron. Here, n_0, b, and E_0 denote the average electron density, microbunch factor satisfying $|b| \leq 1$, and field amplitude, respectively. In the particular condition under consideration, $f(t)$ and $g(t)$ refer to a chirped sinusoid.

The condition that the slippage length at the n-th period is identical to the n-th microbunch interval, is mathematically given by $g(t) = f(T - t)$, where T is an arbitrary time. Redefining the origin of time, we have $E(t) = bn_0 E_0 \mathscr{F}^{-1}[|\tilde{f}(\omega)|^2]$, where $\mathscr{F}^{-1}$ denotes the inverse Fourier transform, and $\tilde{f}(\omega)$ is the Fourier transform of $f(t)$. The above formula means that $E(t)$ is given by the inverse Fourier transform of the spectrum of radiation emitted in the tapered undulator, i.e., $|\tilde{f}(\omega)|^2$. Because $|\tilde{f}(\omega)|^2$ is a slowly varying real function of ω with a wide bandwidth depending on the taper rate, it is obvious that the temporal width of $E(t)$ can be reduced by increasing the bandwidth of $|\tilde{f}(\omega)|^2$, or the chirp rate of CM.

4. Application to FEL Systems

Although the fundamental mechanism to realize the monocycle FELs as explained in the previous section is simple, it is not straightforward to apply the principle to the actual FEL system. The critical issue is how to prepare CM; up to now, two schemes have been proposed, which are explained in the following sections. Note that both of them require a monocycle (or a few-cycle) pulse as seed light, and are similar to what is known as the high gain harmonic generation (HGHG) FELs. The main function is to upconvert the input monocycle seed pulse (with the wavelength of λ_i) to generate shorter-wavelength (λ_o) monocycle pulse, whose pulse length is much shorter than that of the seed monocycle pulse, i.e., $\lambda_o \ll \lambda_i$. Thus the scheme is referred to as monocycle harmonic generation (MCHG).

4.1. *Original Scheme*

Figure 3 shows the accelerator layout to implement the method to control the pulse length by CM in the actual FEL system[5], where respective elements are divided into five sections from (i) to (v), according to their functions. In insets (a)∼(f), the current profile (j, dashed lines) and field profile (E, solid lines) at the entrance and exit of each section are schematically illustrated.

In the initial condition (a), the electron current is constant, and the field profile of radiation corresponds to that of the monocycle seed pulse. By injecting both of them to section (i), i.e., a single period undulator (modulator 1) followed by a magnetic chicane called a dispersive section, a single microbunch is created in the electron beam (b). It should be noted that this microbunch is much shorter than λ_i; to be specific, it contains many high harmonic components. Then, the single microbunch is injected to section (ii), i.e., a tapered undulator (radiator 1) to generate a chirped radiation pulse (c), whose central wavelength corresponds to that

6
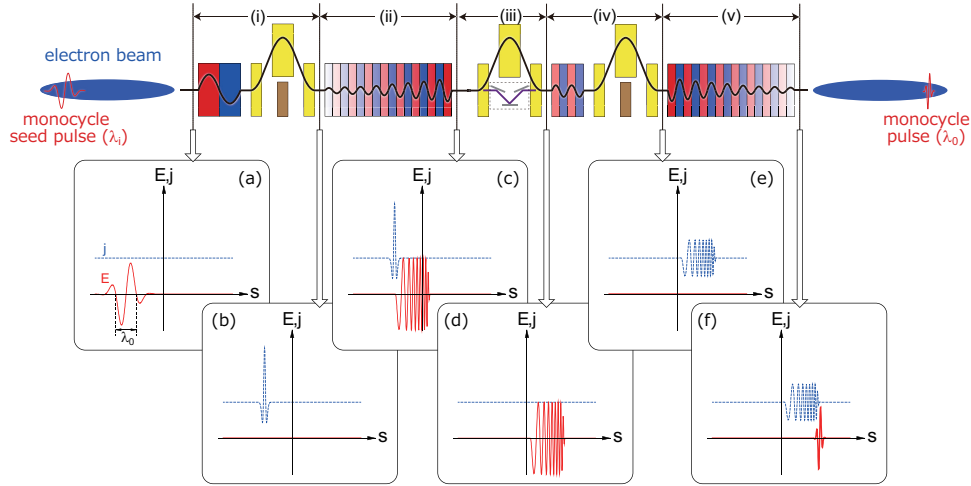
Fig. 3.   Schematic layout of MCHG based on CM.

of the m-th harmonic of the seed pulse (λ_i/m). After passing through the dispersive section (iii), the single microbunch, which is no longer necessary, is washed out (d). Then in section (iv), i.e., the few-period undulator (modulator 2) followed by the dispersive section, CM is created in the electron beam by the chirped pulse (e). Then in section (v), i.e., the tapered undulator (radiator 2) having the same taper rate as the radiator 1, CM emits a monocycle pulse (f) because of the mechanism explained in the previous section. It should be noted that the taper gradient in the radiator 2 is flipped with respect to the radiator 1.

Table 1.   Parameters of the electron beam and monocycle seed pulse assumed in the simulations. Note that the energy spread values assumed in sections 4.1 and 4.2 are different.

Electron Beam		
Energy	2	GeV
Current	2	kA
Normalized Emittance	0.4	mm·mrad
RMS Energy Spread (sec.4.1/4.2)	$0.5/1 \times 10^{-4}$	
Average Betatron Function	4	m
Monocycle Seed Pulse		
Pulse Energy	10	μJ
FWHM Pulse Length	0.38	fs
Central Wavelength	60	nm

To verify the effectiveness of the proposed scheme, numerical simulations have been performed with the parameters of the electron beam and monocycle seed pulse summarized in Table 1. As an example, undulator parameters have been optimized so that the 7th harmonic of the monocycle seed pulse with the central wavelength

of 60 nm is generated in the radiator 2. The simulation results are summarized in Figs. 4(a)∼(d). The current profile of the electron beam at the exit of section (i), where a single microbunch is formed, is shown in Fig. 4(a), while the chirped pulse emitted by this single microbunch, when the electron beam passes through the radiator 1, is plotted in Fig. 4(b). Figure 4(c) shows the current profile at the exit of section (iv), where CM is formed. The final results are shown in Fig. 4(d), where the temporal profiles of the monocycle pulse emitted at the radiator 2 are plotted in terms of the on-axis radiation field and the total radiation power. Note that the FWHM pulse length is 46 as in this example, which corresponds to 1.6 cycles of radiation with the central wavelength of 60/7∼8.6 nm.
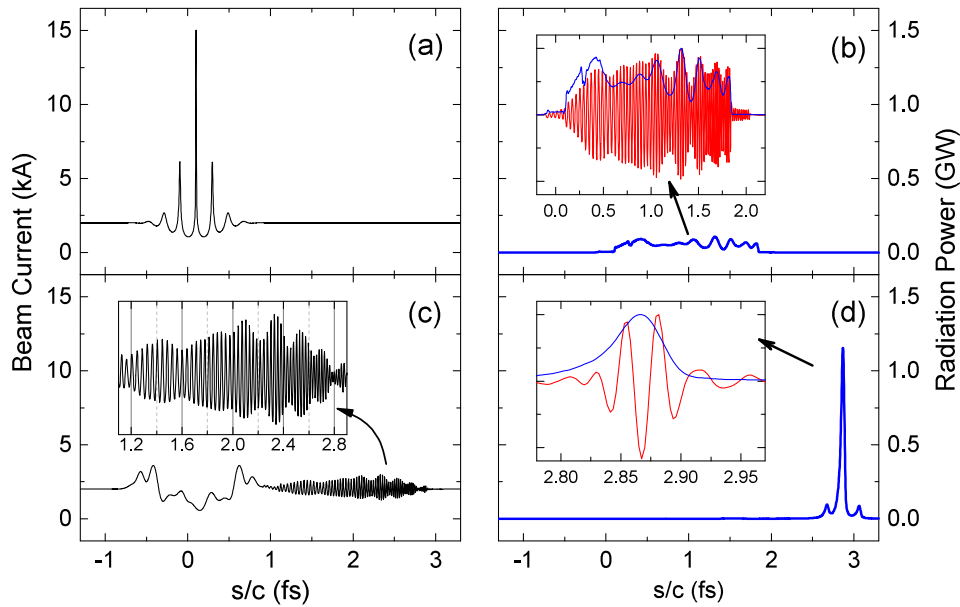
Fig. 4.   Results of simulations to evaluate the performances of MCHG based on CM.

Although this scheme can potentially be a solution toward realization of the monocycle FELs, it has two difficulties for practical applications. One is that the accelerator layout is complicated. The other is that the performance of the output monocycle pulse is extremely sensitive to the energy spread of the electron beam in terms of the radiation power and the pulse length. This is the reason why a small value of 5×10^{-5} has been assumed as the energy spread in the above example; the expected performance has been found to be degraded by more than one order of magnitude in terms of the peak power and pulse length, if the energy spread is doubled.

8

4.2. *Improved Scheme*

The two difficulties in the original scheme mentioned in the previous section come from the fact that CM with the average interval of λ_i/m, where m is the target harmonic number, cannot be directly created by the monocycle seed pulse with the central wavelength of λ_i. As a result, we need to insert an intermediate process to create the chirped pulse with the central wavelength of λ_i/m, which is then used to create CM. As a result, the intensity of the monocycle seed pulse, however strong it is, has almost nothing to do with the performance of the output monocycle pulse. In addition, we need many sections from (i) to (iv), just to prepare CM.

To overcome the difficulties mentioned above, and to improve the upconversion efficiency, an alternative scheme has been proposed[6]. The layout is schematically illustrated in Fig. 5, where only three components are necessary: two tapered undulators and a dispersive section inserted in between.
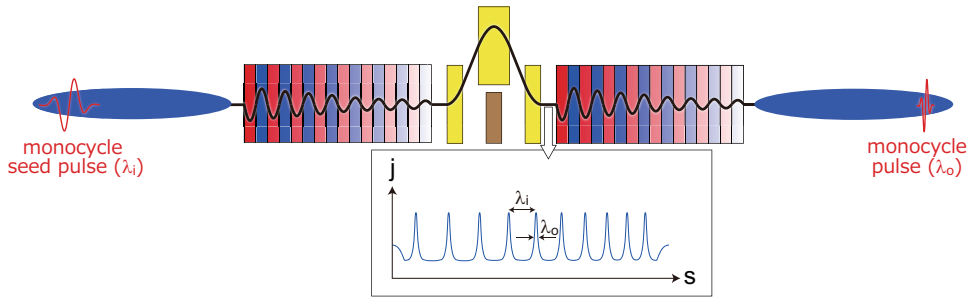
Fig. 5.   Schematic layout MCHG based on HFCM.

The basic idea is to create CM directly by interaction with the monocycle seed pulse in the 1st tapered undulator (modulator) followed by a dispersive section. This results in a current profile shown in inset; local bunches with the length $\lambda_o \ll \lambda_i$ are arranged with intervals linearly changing, and their average is roughly given by λ_i. In other words, the current profile contains high-frequency components and thus such CM is referred to as high-frequency CM (HFCM). Mathematically, the current profile of HFCM is given by

$$f(t) = \sum_{n=1}^{\infty} c_n S(\lambda_i/nc, t - t_n),$$

where $S(T,t)$ is a function to represent a chirped sinusoid with the mean period of T. The parameters c_n and t_n correspond to the amplitude and phase of the n-th harmonic component. The above formula is in contrast to that of normal CM discussed in the previous section, which is simply given by

$$f(t) = S(\lambda_i/mc, t),$$

where m is the target harmonic number.

The pulse lengthening due to the optical slippage can be suppressed even with HFCM, as long as the condition $g(t) = f(T - t)$ is satisfied. Namely, an intense monocycle pulse will be generated when it passes through the 2nd tapered undulator (radiator), if the field profile of radiation emitted by a single electron in the radiator is similar to the current profile of HFCM. This condition is actually satisfied if the 1st and 2nd tapered undulators have the identical specifications, and the magnetic field of them is strong enough. This is a consequence of the fact that the waveform of radiation emitted from a single electron passing through a tapered undulator is in general composed of chirped sinusoids with many high harmonics. Note that the tapered undulator should be a planar type but not a helical one, because the radiation emitted in the forward direction from a helical undulator does not contain any high harmonic components [7].

To illustrate the expected performance of this scheme, simulations have been performed with the parameters summarized in Table 1; note that the energy spread is double of that used in section 4.1, which is more realistic. Figure 6 shows the simulation results in terms of (a) the spectrum, (b)∼(d) temporal profiles of the on-axis field, on-axis power density, and total radiation power, respectively.
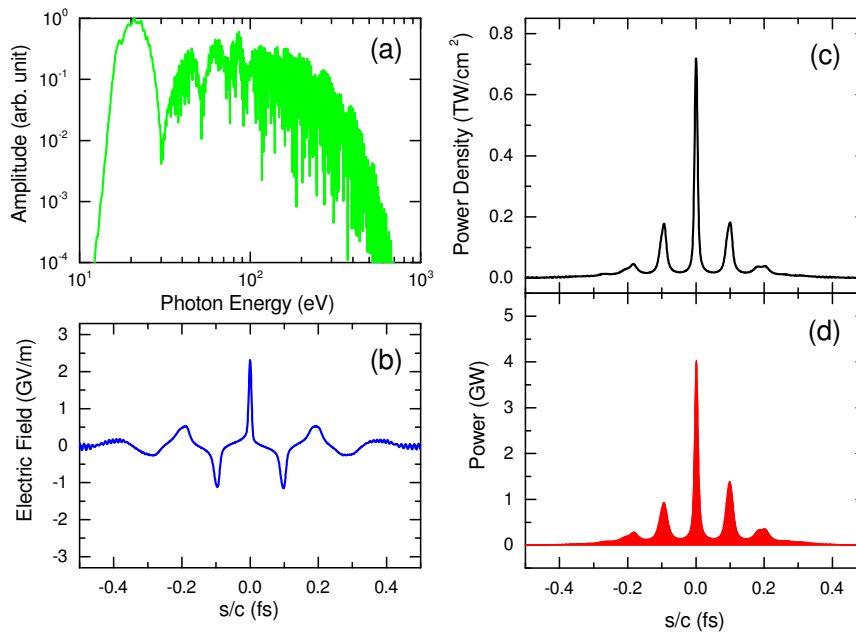
Fig. 6.   Results of simulations to evaluate the performances of MCHG based on HFCM (courtesy of Y. Kida [6]).

As expected from the qualitative discussion, the spectrum of radiation is extremely wideband, and thus the electric field oscillation within the main pulse is

10

less than a half cycle. In other words, a subcycle pulse is generated, with the peak power reaching 4 GW and the FWHM pulse length of 13 as.

It should be noted that the main pulse is surrounded by non-negligible satellite pulses, which can have some impacts on pump-probe experiments using the subcycle pulses generated by this scheme, which is attributable to that the condition $g(t) = f(T - t)$ is not completely satisfied; it is known that the radiation from a conventional planar undulator consists of only odd-number harmonics, while HFCM contains even-number harmonics as well as odd ones. This suggests that the satellite pulses can be eliminated or at least weakened by using a specially designed tapered undulator as the radiator.

In the above example, HFCM is assumed to be created by a monocycle seed pulse combined with a tapered undulator. It is worth noting that another scheme, i.e., a chirped pulse combined with a few-period undulator, is also possible, which may be more feasible just for creating HFCM. In this case, however, the radiator specification and configuration may be more complicated so that the condition $g(t) = f(T - t)$ is satisfied.

5. Summary

In this paper, we have explained the fundamental mechanism to counteract the pulse lengthening due to the optical slippage in FELs, and reviewed a few schemes to realize monocycle FELs proposed so far, together with several numerical examples. Although the wavelength of the output monocycle pulse in these example is in the soft x-ray regions, it is expected that the wavelength and pulse length can be shorter, by shortening the wavelength of the monocycle seed pulse, enhancing its intensity, and increasing the electron energy if necessary. In practice, the performance of the monocycle pulse generated by the HHG scheme is being improved year by year in terms of the pulse length and intensity. It is thus reasonable to say that the proposed scheme and HHG are not competing, but can collaborate with each other to promote the development of short pulse lasers.

We finally stress that the proposed scheme can be cascaded, for further shortening the pulse length. Namely, a monocycle pulse with even shorter wavelengths can be generated by using the output monocycle pulse generated in the 1st stage as the monocycle seed pulse in the 2nd stage. This gives us a possibility to generate a monocycle pulse in the hard x-ray regions with the pulse length reaching the zeptosecond regions. It goes without saying that realization of such an extremely short and intense pulse definitely contributes to investigation of unresolved ultrafast dynamics.

References

1. L. N. M. Sansone, Giuseppeand Poletto, High-energy attosecond light sources, *Nature Photonics* **5**, 655 (Nov 2011).
2. P. Emma, R. Akre, J. Arthur, R. Bionta, C. Bostedt, J. Bozek, A. Brachmann,

P. Bucksbaum, R. Coffee, F.-J. Decker, Y. Ding, D. Dowell, S. Edstrom, A. Fisher, J. Frisch, S. Gilevich, J. Hastings, G. Hays, P. Hering, Z. Huang, R. Iverson, H. Loos, M. Messerschmidt, A. Miahnahri, S. Moeller, H.-D. Nuhn, G. Pile, D. Ratner, J. Rzepiela, D. Schultz, T. Smith, P. Stefan, H. Tompkins, J. Turner, J. Welch, W. White, J. Wu, G. Yocky and J. Galayda, First lasing and operation of an angstrom-wavelength free-electron laser, *Nature Photonics* **4**, 641 (Sep 2010).

3. E. Allaria, R. Appio, L. Badano, W. A. Barletta, S. Bassanese, S. G. Biedron, A. Borga, E. Busetto, D. Castronovo, P. Cinquegrana, S. Cleva, D. Cocco, M. Cornacchia, P. Craievich, I. Cudin, G. D'Auria, M. Dal Forno, M. B. Danailov, R. De Monte, G. De Ninno, P. Delgiusto, A. Demidovich, S. Di Mitri, B. Diviacco, A. Fabris, R. Fabris, W. Fawley, M. Ferianis, E. Ferrari, S. Ferry, L. Froehlich, P. Furlan, G. Gaio, F. Gelmetti, L. Giannessi, M. Giannini, R. Gobessi, R. Ivanov, E. Karantzoulis, M. Lonza, A. Lutman, B. Mahieu, M. Milloch, S. V. Milton, M. Musardo, I. Nikolov, S. Noe, F. Parmigiani, G. Penco, M. Petronio, L. Pivetta, M. Predonzani, F. Rossi, L. Rumiz, A. Salom, C. Scafuri, C. Serpico, P. Sigalotti, S. Spampinati, C. Spezzani, M. Svandrlik, C. Svetina, S. Tazzari, M. Trovo, R. Umer, A. Vascotto, M. Veronese, R. Visintini, M. Zaccaria, D. Zangrando and M. Zangrando, Highly coherent and stable pulses from the FERMI seeded free-electron laser in the extreme ultraviolet, *Nature Photonics* **6**, 699 (Oct 2012).

4. T. Ishikawa, H. Aoyagi, T. Asaka, Y. Asano, N. Azumi, T. Bizen, H. Ego, K. Fukami, T. Fukui, Y. Furukawa, S. Goto, H. Hanaki, T. Hara, T. Hasegawa, T. Hatsui, A. Higashiya, T. Hirono, N. Hosoda, M. Ishii, T. Inagaki, Y. Inubushi, T. Itoga, Y. Joti, M. Kago, T. Kameshima, H. Kimura, Y. Kirihara, A. Kiyomichi, T. Kobayashi, C. Kondo, T. Kudo, H. Maesaka, X. M. Marechal, T. Masuda, S. Matsubara, T. Matsumoto, T. Matsushita, S. Matsui, M. Nagasono, N. Nariyama, H. Ohashi, T. Ohata, T. Ohshima, S. Ono, Y. Otake, C. Saji, T. Sakurai, T. Sato, K. Sawada, T. Seike, K. Shirasawa, T. Sugimoto, S. Suzuki, S. Takahashi, H. Takebe, K. Takeshita, K. Tamasaku, H. Tanaka, R. Tanaka, T. Tanaka, T. Togashi, K. Togawa, A. Tokuhisa, H. Tomizawa, K. Tono, S. Wu, M. Yabashi, M. Yamaga, A. Yamashita, K. Yanagida, C. Zhang, T. Shintake, H. Kitamura and N. Kumagai, A compact X-ray free-electron laser emitting in the sub-angstrom region, *Nature Photonics* **6**, 540 (Aug 2012).

5. T. Tanaka, Proposal to generate an isolated monocycle x-ray pulse by counteracting the slippage effect in free-electron lasers, *Phys. Rev. Lett.* **114**, p. 044801 (Jan 2015).

6. Y. Kida, R. Kinjo and T. Tanaka, Synthesizing high-order harmonics to generate a sub-cycle pulse in free-electron lasers, *Applied Physics Letters* **109**, p. 151107 (2016).

7. B. M. Kincaid, A shortperiod helical wiggler as an improved source of synchrotron radiation, *Journal of Applied Physics* **48**, 2684 (1977).